Electronic Supplementary Material (ESI) for Journal of Materials Chemistry A.

A Novel P3-type $Na_{2/3}Mg_{1/3}Mn_{2/3}O_2$ as High Capacity Sodium-Ion Cathode Using Reversible Oxygen Redox

Bohang Song,[1] Enyuan Hu,[2] Jue Liu,[1,*] Yiman Zhang,[3] Xiao-Qing Yang,[2] Jagjit Nanda,[3] Ashfia Huq,[1,*] Katharine Page,[1,*]

[1] *Neutron Scattering Division, Oak Ridge National Laboratory, Oak Ridge, Tennessee 37831, United States*

[2] *Chemistry Division, Brookhaven National Laboratory, Upton, New York 11973, United States*

[3] *Materials Science and Technology Division, Oak Ridge National Laboratory, Oak Ridge, Tennessee 37831, United States*

** Corresponding author: liuj1@ornl.gov, huqa@ornl.gov, pagekl@ornl.gov*

Table S1. Rietveld refinement of the structure of the P3-type $Na_{2/3}Mg_{1/3}Mn_{2/3}O_2$ using S.G. *R*3m (λ = 0.412748 Å)

S.G. *R*3m		a = 2.8980(1) Å, c = 16.7883(5) Å				
Site	Wyck.	x	y	z	Occ.	B_{iso} (Å^2)
Mn	3a	0	0	0	0.974(3)	0.08(1)
Mg	3a	0	0	0	0.026(3)	0.08(1)
Na	3a	0	0	0.1712(2)	0.529(4)	1.52(9)
O1	3a	0	0	0.3922(5)	1	0.8
O4	3a	0	0	0.6022(5)	1	0.8

Table S2. Refined Mg/Mn ordered local structure (S.G. *C*m) of P3-type $Na_{2/3}Mg_{1/3}Mn_{2/3}O_2$ using neutron PDF data (1-8 Å)

S.G. *C*m		a = 5.0750(46) Å, b = 8.6476(60) Å, c = 5.8215(36) Å, β = 106.47(58)°				
Site	Wyck.	x	y	z	Occ.	B_{iso} (Å^2)
Mn1	4b	0.5124(9)	0.1633(5)	0	0.99(1)	0.19(2)
Mg1	4b	0.5124(9)	0.1633(5)	0	0.00(1)	0.22(2)
Mn2	2a	0	0	0	0.01(2)	0.19(2)
Mg2	2a	0	0	0	0.99(2)	0.22(2)
Na1	2a	0.1969(66)	0	0.5	0.63(2)	2.72(26)
Na2	4b	0.6822(66)	0.1534(28)	0.5	0.63(2)	2.72(26)
O1	2a	0.4230(12)	0	0.1580(11)	1	0.53(3)
O2	2a	0.6056(11)	0	0.8141(11)	1	0.53(3)
O3	4b	0.3867(8)	0.3245(5)	0.1790(11)	1	0.51(2)
O4	4b	0.6211(10)	0.3184(4)	0.7972(8)	1	0.51(2)

Table S3. Refined O3 phase for the half charged sample using synchrotron XRD (λ = 0.412748 Å)

S.G. *R*-3m		a = 2.8673(3) Å, c = 15.0250(63) Å				
Site	Wyck.	x	y	z	Occ.	B_{iso} (Å^2)
Mn	3b	0	0	0.5	0.761(6)	0.3
Mg_{tetra}	6c	0	0	0.6235(25)	0.110(5)	0.3
Na	3a	0	0	0	0.350(11)	2

O	6c	0	0	0.2306(4)	1	0.8

Table S4. Refined O3 phase for the 4.4 V charged sample using synchrotron XRD (λ = 0.412748 Å)

S.G. *R*-3m		a = 2.8649(5) Å, c = 14.6612(34) Å				
Site	Wyck.	x	y	z	Occ.	B_{iso} (Å^2)
Mn	3b	0	0	0.5	0.547(3)	0.3
Mg_{tetra}	6c	0	0	0.6200(9)	0.158(2)	0.3
Na	3a	0	0	0	0.001(3)	2
O	6c	0	0	0.2383(2)	1	0.8

Table S5. Refined O3 phase for the 2.75 V discharged sample using synchrotron XRD (λ = 0.412748 Å)

S.G. *R*-3m		a = 2.8713(2) Å, c = 15.5330(25) Å				
Site	Wyck.	x	y	z	Occ.	B_{iso} (Å^2)
Mn	3b	0	0	0.5	0.651(5)	0.3
Mg_{tetra}	6c	0	0	0.6201(9)	0.119(2)	0.3
Na	3a	0	0	0	0.311(5)	2
O	6c	0	0	0.2333(2)	1	0.8

Table S6. Refined O3 phase for the 2.1 V discharged sample using synchrotron XRD (λ = 0.412748 Å)

S.G. *R*-3m		a = 2.9082(2) Å, c = 16.3244(23) Å				
Site	Wyck.	x	y	z	Occ.	B_{iso} (Å^2)
Mn	3b	0	0	0.5	0.818(7)	0.3
Mg_{tetra}	6c	0	0	0.6379 (4)	0.032(2)	0.3
Na	3a	0	0	0	0.612(6)	2
O	6c	0	0	0.2345(2)	1	0.8

Table S7. Refined O3 phase for the 1.6 V discharged sample using synchrotron XRD (λ = 0.412748 Å)

S.G. *R*-3m		a = 2.9428(8) Å, c = 16.1836(58) Å				
Site	Wyck.	x	y	z	Occ.	B_{iso} (Å^2)
Mn	3b	0	0	0.5	0.823(6)	0.3
Mg_{tetra}	6c	0	0	0.610(11)	0.007(4)	0.3
Na	3a	0	0	0	0.785(7)	2
O	6c	0	0	0.2326(2)	1	0.8

Table S8. FT-EXAFS fitted value of the pristine sample.

	coordination number	bond length (Å)	Debye-Waller factor (Å^2)
Mn-O	6	1.9277(14)	0.0018(20)
Mn-Mn	3	2.8557(28)	0.0022(4)
Mn-Mg	3	2.9085(28)	0.0022(4)
Mn-Na	4	2.9728(13)	0.0033(9)

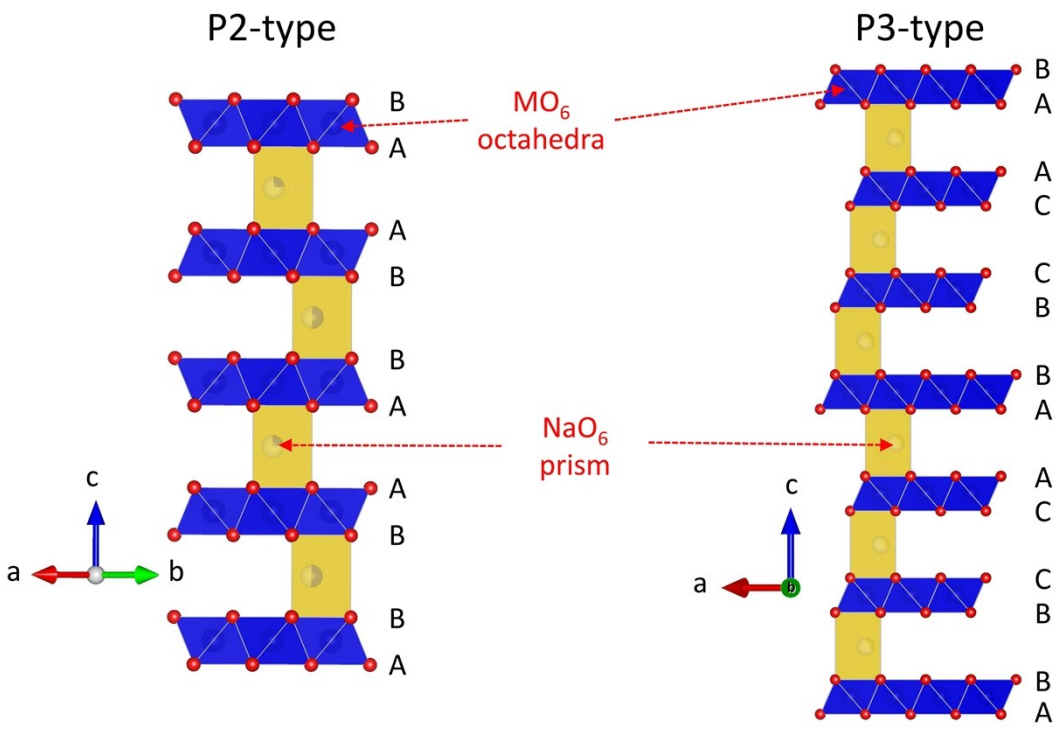

Figure S1. Stacking sequences of the P2- and P3-type sodium transition metal layered oxides.

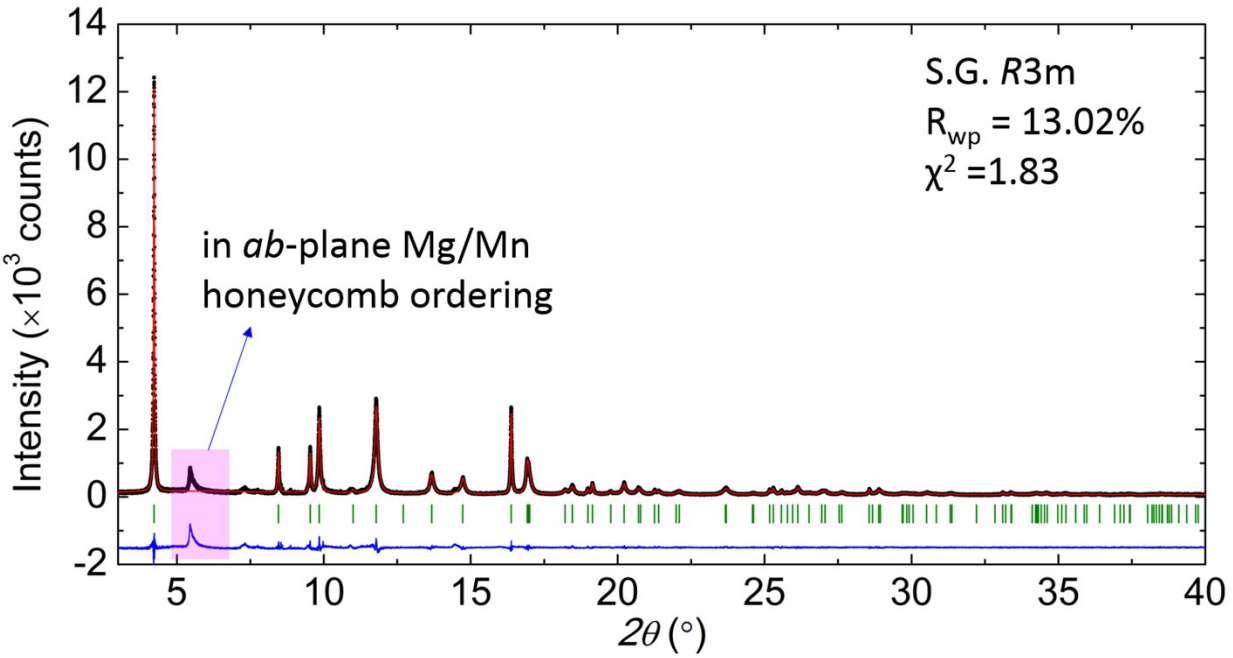

Figure S2. Le Bail fit of the synchrotron XRD data (λ = 0.412748 Å) of the P3-type $Na_{2/3}Mg_{1/3}Mn_{2/3}O_2$ using S.G. *R*3m. The highlighted region shows the diffuse scattering peak caused by the in *ab*-plane Mg/Mn honeycomb ordering.

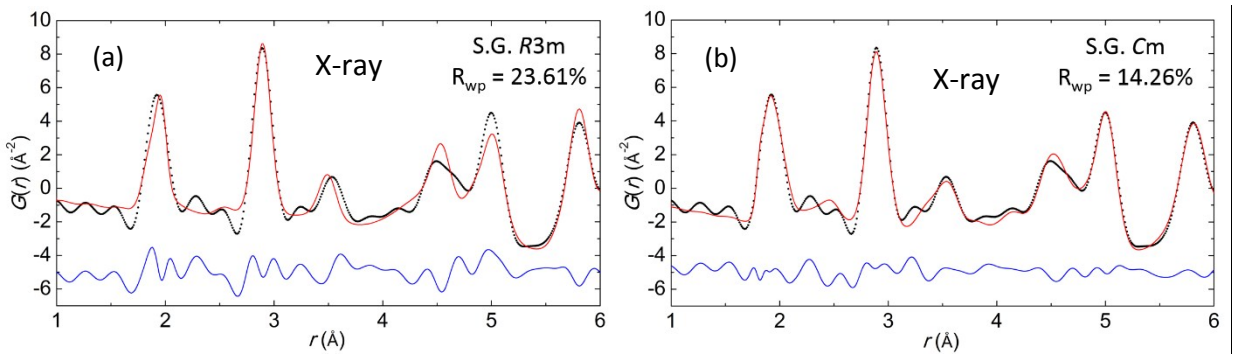

Figure S3. Least square refinements of the Mg/Mn random distribution model (S.G. *R*3m, a) and the in *ab*-plane honeycomb ordered model (S.G. *C*m, b) using short range X-ray PDF data (1-6 Å).

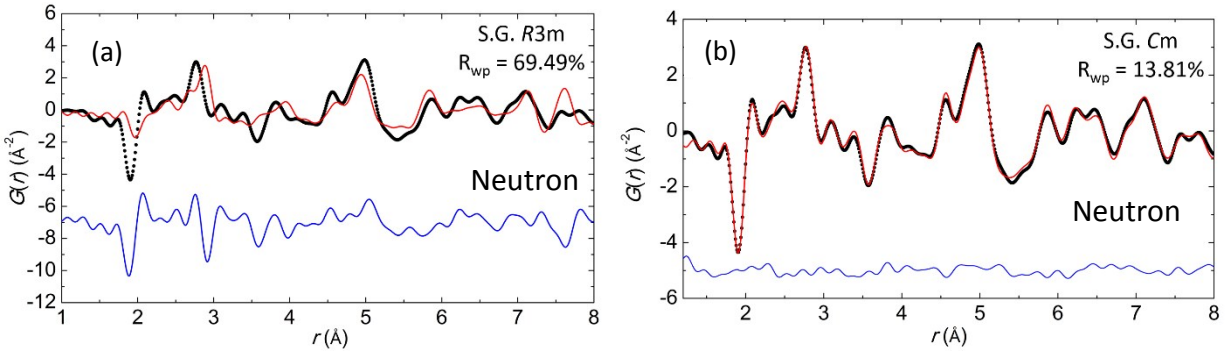

Figure S4. Least square refinements of the Mg/Mn random distribution model (S.G. *R*3m, a) and the in *ab*-plane honeycomb ordered model (S.G. *C*m, b) using short range neutron PDF data (1-8 Å).

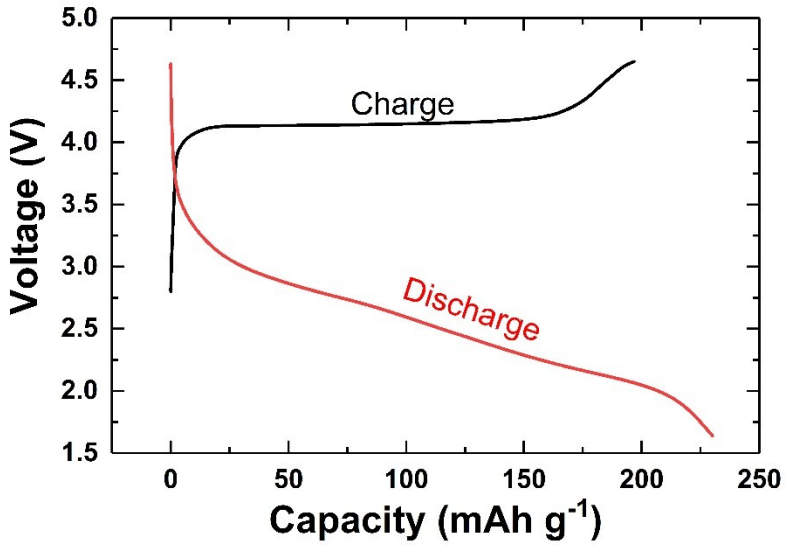

Figure S5. The initial Galvanostatic charge and discharge of the P3-type $Na_{2/3}Mg_{1/3}Mn_{2/3}O_2$ between 1.6 V and 4.65 V with a rate of C/20.

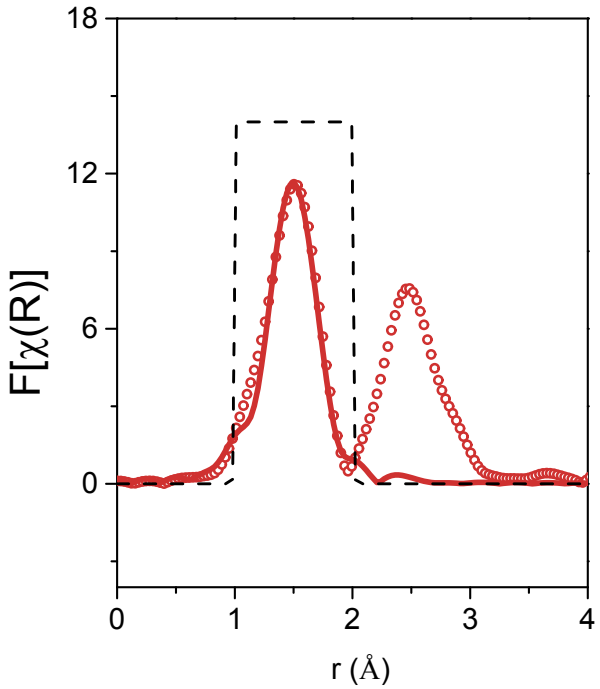

Figure S6. FT-EXAFS fitting of the first peak by using two paths (two Mn-O bond lengths) for the first Mn-O shell of P3-type $Na_{2/3}Mg_{1/3}Mn_{2/3}O_2$. It is much better fitted than using just one path (one Mn-O bond lengths), indicating dramatic local distortion of MnO_6 octahedra.

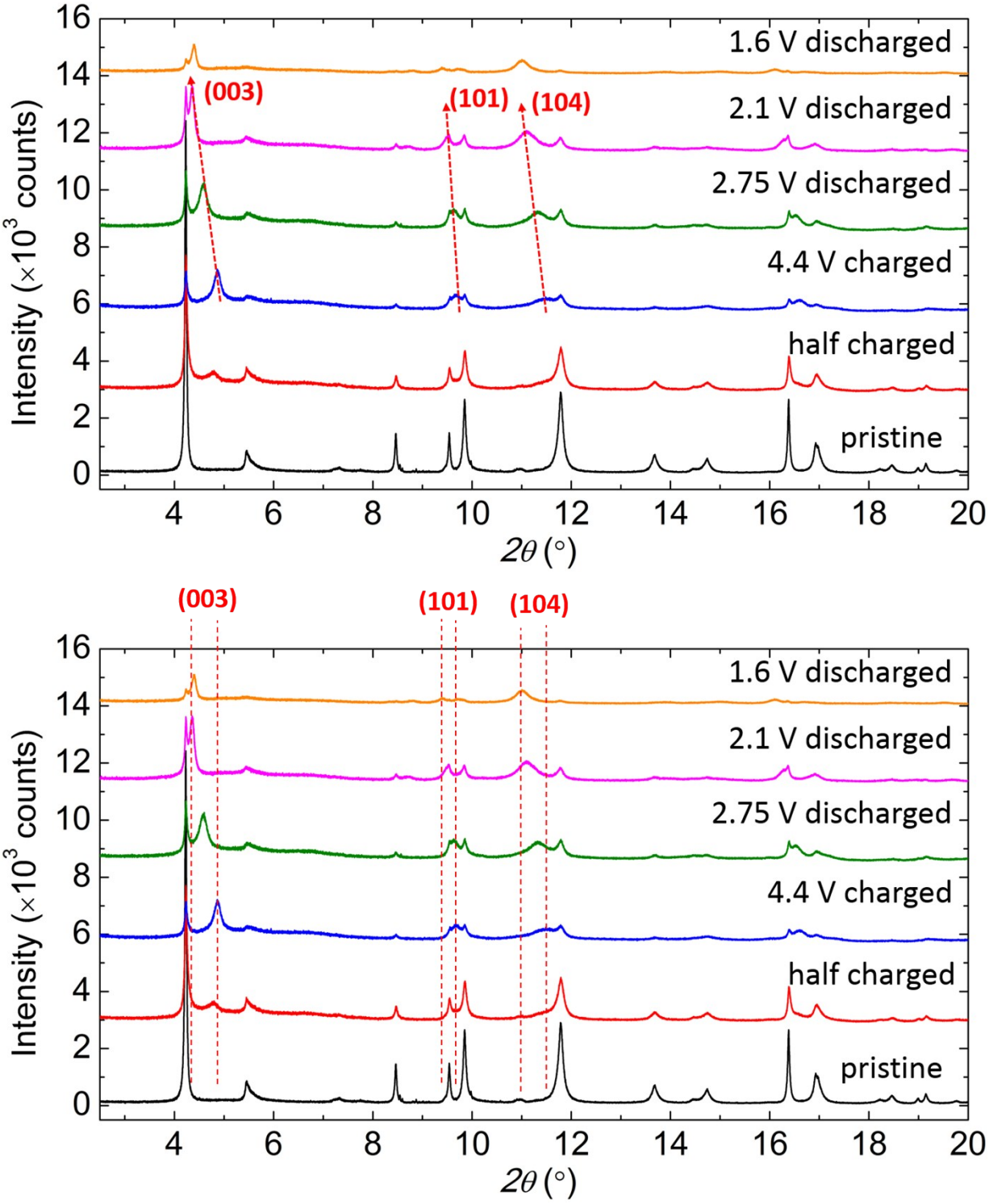

Figure S7. *Ex situ* high resolution XRD (λ = 0.412748 Å) patterns of the P3-type $Na_{2/3}Mg_{1/3}Mn_{2/3}O_2$ at different charge and discharge states. The first three major reflections, i.e. 003, 101 and 104, of the O3 phase are labeled.

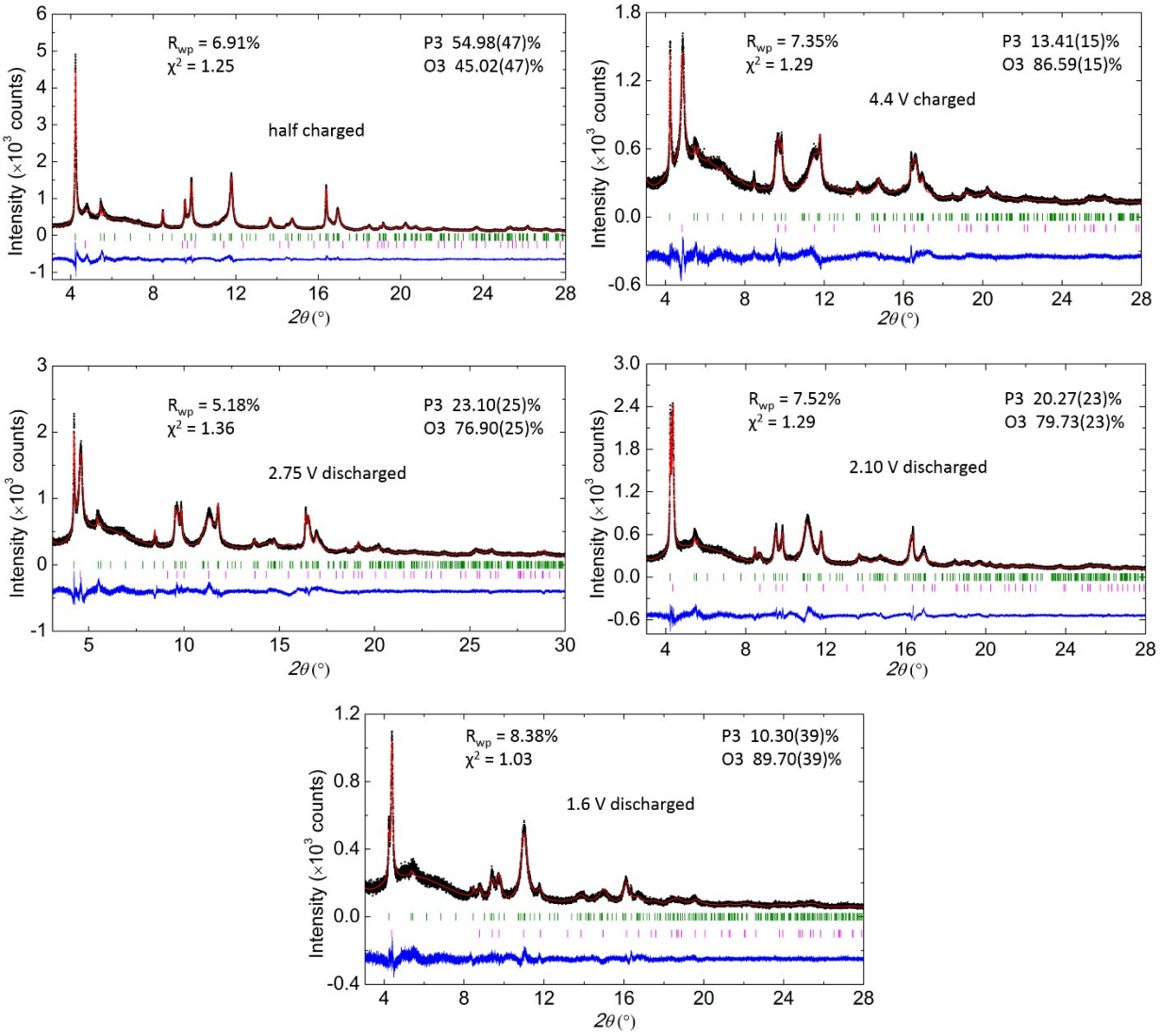

Figure S8. Rietveld refinement of P3-type $Na_{2/3}Mg_{1/3}Mn_{2/3}O_2$ at different charge and discharge states (half charged, 4.4 V charged, 2.75 V discharged, 2.1 V discharged and 1.6 V discharged) using high resolution synchrotron XRD (λ = 0.412748 Å). The experimental data are shown in black dots, calculated data in red and difference curves in blue. The Bragg reflections of the P3 and O3 phases are marked with green and pink markers separately.

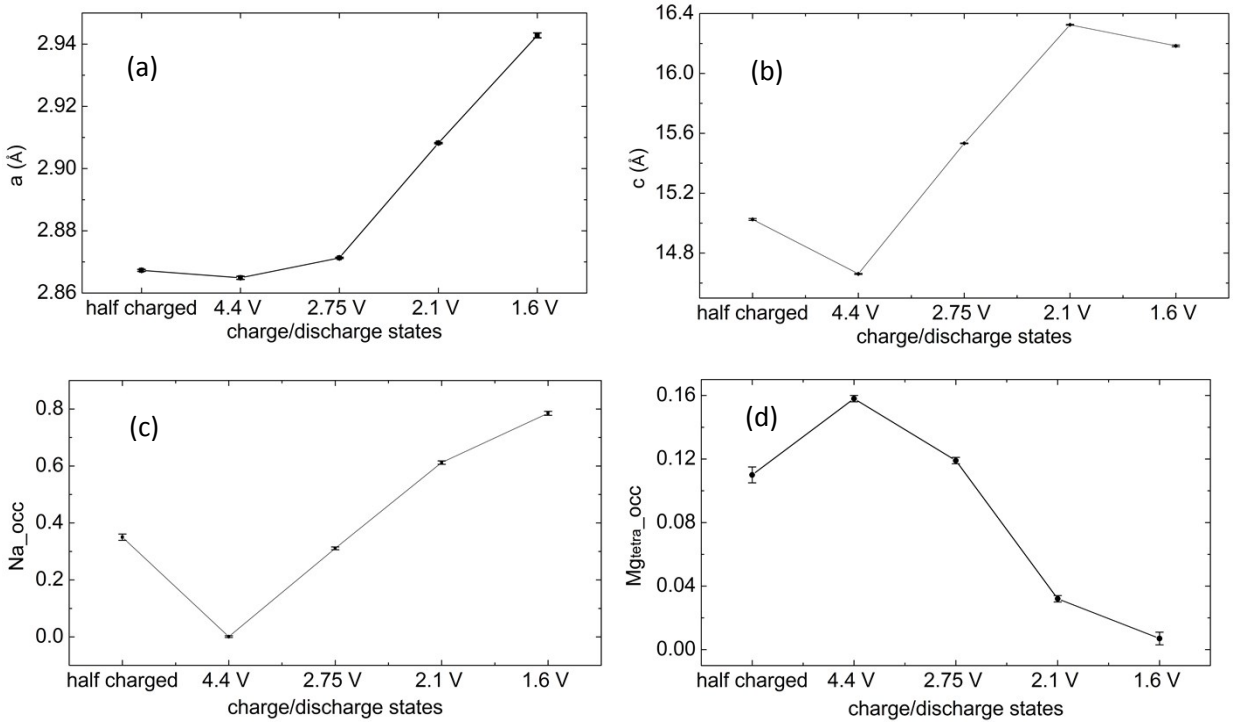

Figure S9. Refined lattice parameters a (a) and c (b) of the O3 phase at different charge and discharge states. The refined site occupancies for sodium and tetrahedral site magnesium of the O3 phase at different charge and discharge states.